Tertiary and secondary control levels for efficiency optimization and system damping in droop controlled dc-dc converters

Meng, Lexuan; Dragicevic, Tomislav; Quintero, Juan Carlos Vasquez; Guerrero, Josep M.

Published in:
I E E E Transactions on Smart Grid

DOI (link to publication from Publisher):
10.1109/TSG.2015.2435055

Publication date:
2015

Document Version
Early version, also known as pre-print

Tertiary and Secondary Control Levels for Efficiency Optimization and System Damping in Droop Controlled DC-DC Converters

Lexuan Meng, *Student Member, IEEE*, Tomislav Dragicevic, *Member, IEEE*, Juan C. Vasquez, *Senior Member, IEEE* and Josep M. Guerrero, *Fellow, IEEE*

***Abstract*-- Droop control by means of virtual resistance (VR) control loops can be applied to paralleled dc-dc converters for achieving autonomous equal power sharing. However, equal power sharing does not guarantee an efficient operation of the whole system. In order to achieve higher efficiency and lower energy losses, this paper proposes a tertiary control level including an optimization method for achieving efficient operation. As the efficiency of each converter changes with the output power, VR values are set as decision variables for modifying the power sharing ratio among converters. Genetic algorithm is used in searching for a global efficiency optimum. In addition, a secondary control level is added to regulate the output voltage drooped by the VRs. However, system dynamics is affected when shifting up/down the VR references. Therefore, a secondary control for system damping is proposed and applied for maintaining system stability. Hardware-in-the-loop simulations are conducted to validate the effectiveness of this method. The results show that the system efficiency is improved by using tertiary optimization control and the desired transient response is ensured with system damping secondary control.**

***Index Terms*--tertiary control, efficiency optimization, secondary control, system damping, droop method, hierarchical control, dc-dc converters.**

I. Introduction

Direct current (dc) electricity distribution systems are generally accepted as high efficiency, high reliability and simple control systems [1]–[6]. During last decades, parallel operation of dc-dc converters have been widely used in various applications, such as in dc power conversion systems like shown in Fig. 1, which show many advantages such as enhanced flexibility, reduced thermal and electrical stress, improved reliability and so forth [1]–[3].

For the parallel operation, one challenging issue is the current sharing control among converters. Up to date, several kinds of current sharing approaches have been proposed, and they can be classified as active current sharing techniques and droop methods [1]. The droop control steams from classical power system theories to mimic the nature of synchronous generators which drop their frequency/voltage when active or reactive power demands increase. In paralleled dc/dc converters control system, droop control appears as an external loop, also named virtual resistance (VR) loop, over inner voltage and current control loops [7], [8]. Since droop control is a decentralized strategy which does not require communication links and offers higher reliability and flexibility, it is preferred in paralleled converter systems and distributed power systems [3], [4], [7]–[10].

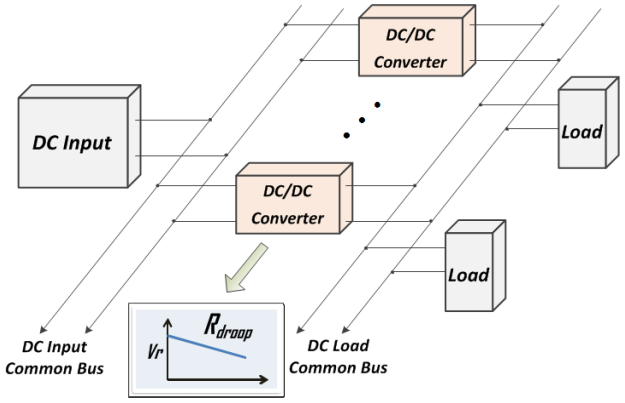

Fig. 1. Droop-controlled dc-dc conversion system

Although the droop control facilitates autonomous power sharing among paralleled converters, in its basic from it does not guarantee an optimum system operation. In order to improve the conversion efficiency, many efforts have been made on enhancing the performance of each single converter [11]–[18]. Especially, it is recognized that converter efficiency is relatively lower in light load conditions where more improvement are expected [15]–[17], [19]. Apart from improving the design and control for a single converter, the system level control strategy for operating all the converters can also be optimized. In [19], an Inverter-Dropping method for enhancing the efficiency of paralleling inverters in light load conditions is proposed. Similarly with this method but instead of dropping modules, this paper proposes a VR shifting method for adjusting operation points of converters so as to optimize the sharing proportion among converters and achieve higher system efficiency. By properly establishing the system mathematical model and designing the interface between tertiary control and lower control levels, the optimization can be performed online.

Lexuan Meng, Tomislav Dragicevic, Josep M. Guerrero, Juan C. Vásquez are with Department of Energy Technology, Aalborg University, 9220 Aalborg (e-mail: lme@et.aau.dk; tdr@et.aau.dk; juq@et.aau.dk; joz@et.aau.dk).

However, stability issues may appear when VRs are changed. In order to ensure system stability, small signal analysis is usually applied in order to find proper control parameters [10], [20]–[23]. In [10], suitable VRs are calculated according to small signal analysis results for keeping stable operation. In [21], a stability margin for droop gains when executing energy management is set. In order to achieve proper load sharing while keeping stable operation especially in high gain angle droop conditions, a supplementary droop control is introduced in [22]. Necessarily, small signal analysis method for ensuring system stability is also studied in this paper, and in additional to that, a secondary control for system damping (SCSD) is proposed achieving automatic desirable system damping control.

A 3-level hierarchical control scheme is proposed in this paper formulating a complete control system. A droop-controlled buck converter based dc-dc conversion system is taken as an example. The structure of hierarchical control method is described in section II, with droop control, bus voltage secondary control, SCSD and tertiary control for efficiency optimization (TCEO) being distinguished. In Section III, the optimization problem is formulated and analyzed by defining the objective function and respective constraints. The algorithm is also presented and tuned. Section IV introduces a novel method of SCSD for desirable system damping. The state-space model of the system is established, root locus analysis is described and the control structure is also presented. In Section V, hardware-in-the-loop (HIL) simulation results are presented and discussed. Finally, Section VI gives the conclusion.

For the sake of simplicity, the analysis has been done for a 2-converter system, and then the HIL simulations are extended to a 4-converter system.

II. Hierarchical Control Architecture

Hierarchical control was proposed for proper control of microgrids [7], [8]. Three control levels, defined as primary control, secondary control and tertiary control, are integrated together to fulfill control objectives in different significances and time scales. The concept of hierarchical control can be conceived in paralleled dc-dc converter system, as shown in Fig. 2. Primary control enables power sharing among converters by using droop control. Secondary control deals with voltage deviation restoration, and in addition to that, this paper also proposes a SCSD method to realize enhanced system dynamics. In the top level, tertiary control was usually issued the task of power flow control. Moreover, optimization functions can be also integrated in this level acting on set-points within the primary and secondary control and achieving optimal operation of the whole system. In this paper, by properly establishing the mathematical model, online optimization is realized.

In Fig. 2, the plant block shows a simplified equivalent circuit of two dc-dc converters connected in parallel powering a common load bus. Droop controlled dc-dc converter acts as a voltage source in series with VR (R_d). In primary level,

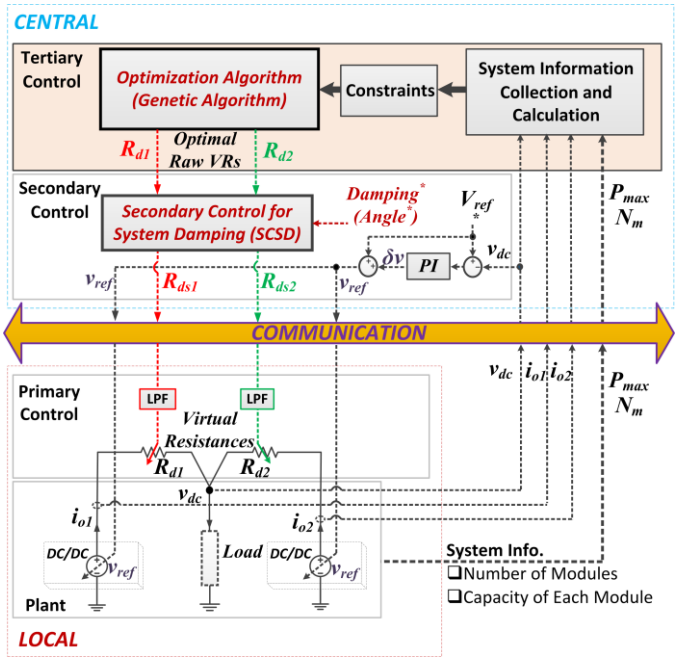

Fig. 2. Hierarchical control applied to dc system

droop control method is implemented which includes the VR control loop expressed as:

$$v_{dc} = v_{ref} - R_d \cdot i_o \tag{1}$$

where i_o is the output current of each unit, R_d is the VR value, and v_{ref} is the output voltage reference at no load. Usually VR is fixed by the maximum allowed voltage deviation ε_v and maximum output current i_{max}:

$$R_d = \varepsilon_v / i_{\max} \tag{2}$$

Primary loop ensures power sharing and stable operation, however, according to (1), the voltage deviation is inherent and depends on load current. In order to solve this problem, voltage secondary control is implemented. The dc bus voltage is sensed and compared with desired voltage V_{ref}^*, with the voltage error being sent to a PI (Proportional-Integral) controller to generate a compensating quantity δv for each converter reference:

$$\delta v = k_p (V_{ref}^* - v_{dc}) + k_i \int (V_{ref}^* - v_{dc}) dt \tag{3}$$

Then the reference voltage with secondary voltage restoration can be generated as:

$$v_{ref} = V_{ref}^* + \delta v \tag{4}$$

Finally, tertiary level receives system data including the number of operating converters, the rated power and output current of each converter. Received information is processed by optimization algorithm to find the optimal load current sharing proportion. VRs are the actual decision variables for adjusting sharing efforts of each converter. However, in order to keep stable operation while changing VRs, a SCSD is implemented to readjust the optimal VRs given by TCEO so as to control the system to a desired damping level. Also, a 1st order butterworth low pass filter (LPF) is required between higher level regulation and primary droop to smooth the

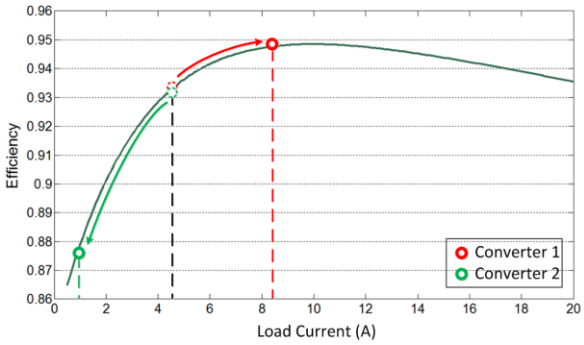

Fig. 3. Typical converter efficiency curve

shifting of VRs, so as to decouple the dynamics of different control levels. Generally, each higher control level needs to be approximately an order of magnitude slower than the down streaming level [7], [24]. Considering that the voltage control loop response time is around 0.02-0.04s, the cut-off frequency of the LPF between tertiary control and lower control levels is set to 5Hz.

It is noteworthy that secondary voltage restoration control (SVRC) is important when considering higher level controls. Without SVRC the voltage deviation caused by droop control and stochastic load changes cannot be fast restored. In this sense, SVRC provides significant support to stabilize dc bus voltage. LPFs are necessarily needed to slow down the change of VR values as well as to decouple the regulation speed of VR adaptive control and SVRC.

III. Optimization Problem Formulation and Analysis

Although modern power electronic system provides high efficiency conversion, losses are inevitable, and minimization of losses is required. In a paralleling converter system, total losses are mostly related to conversion losses which mainly include switching loss of semiconductor components and conduction loss of parasitic resistive elements [25]–[27]. Since these losses are related with conversion current, even if constant input and output voltages are assumed, converter efficiency changes with its load current as shown in Fig. 3 [17], [25]–[29]. The highest efficiency is usually reached between 30% to 60% load (the power losses change with conversion current nonlinearly), there exists a room for optimization, which is to find the power sharing proportion where the losses of the system are minimum.

A. Converter Efficiency and Objective Function

A theoretical efficiency curve is shown in Fig. 3. *Matlab Curve Fitting Tool* is used to transform data into function:

$$\eta(i) = 0.975 \cdot e^{-2\times10^{-3}\cdot i} - 0.1257 \cdot e^{-0.3\cdot i} \tag{5}$$

where η is converter efficiency and i is converter output current. Then, the power conversion losses of a system with n paralleled converters may be calculated as follows:

$$P_{TL} = \sum_{j=1}^{n} V_{DC} \cdot I_j \cdot \frac{1-\eta_j}{\eta_j} \tag{6}$$

where V_{DC} is dc bus voltage, I_j is the output current of j^{th} converter, and η_j is the efficiency of j^{th} converter. Minimization of total conversion losses, P_{TL}, is taken as the objective in the following optimization problem.

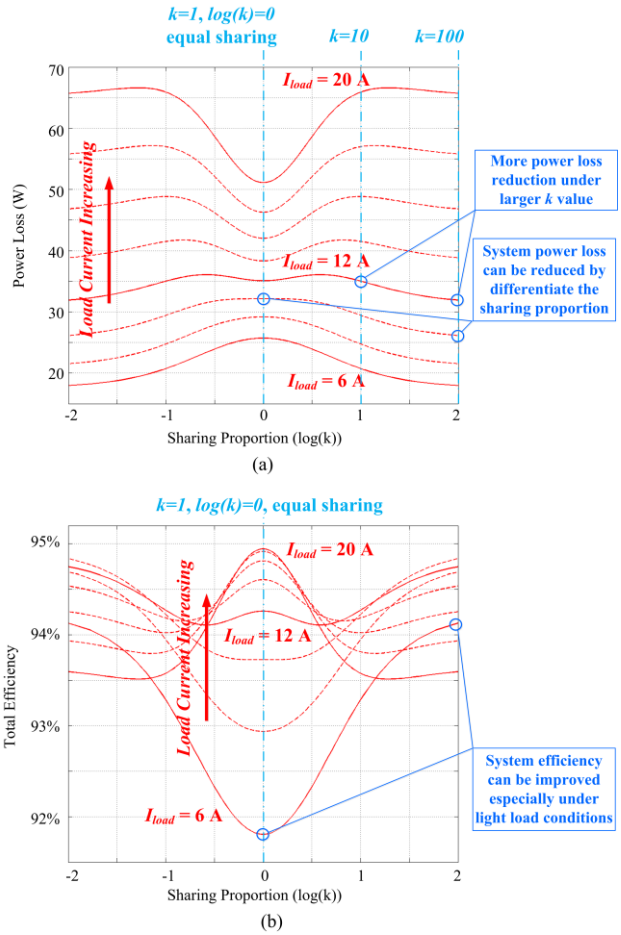

Fig. 4. The effect of sharing proportion changing: (a) system power loss changing with sharing proportion; (b) system efficiency changing with sharing proportion.

Assuming two converters operating in parallel with the same efficiency curve, as shown in Fig. 3, the general approach for enhancing system efficiency is to differentiate sharing proportion in light load conditions instead of equal sharing load current. A sharing proportion gain k is defined as:

$$\begin{cases} k = \dfrac{I_1}{I_2} \\ I_1 + I_2 = I_{load} \end{cases} \tag{7}$$

which is used to evaluate the system power loss and efficiency change, as shown in Fig. 4.

Fig. 4 (a) and (b) shows the varying trends of system power losses and total efficiency with sharing proportion in different load current levels. In light load condition (I_{load} = 6A), the system loss is lower when the sharing proportion gain is higher while in heavy load condition (I_{load} = 20A) the system loss is lower when the two converters equally share the load current. The physical intuition behind the phenomenon is that, if the two converters are equally sharing the load current, the system overall efficiency is the average efficiency between the converters, while if the sharing ratio is differentiated, the

system overall efficiency is mostly decided by the converter which is supplying most of the load current (since most of the power loss is caused by the one which supplies most load current). As can be seen from the typical efficiency curve in Fig. 3, in light load condition, the efficiency of the converter is low, if the two converters equal share load current, the system overall efficiency is the average efficiency between them (dashed red and green points in Fig. 3). Alternatively, one of them can supply most of the load current with high efficiency, while the other one outputs little current. The system overall efficiency is close to the efficiency of the converter that supplies most of the load current (solid red point in Fig. 3), which is obviously much higher than average sharing condition. As a result, it can be seen in Fig. 4 that in light load condition the system efficiency is lower when k=1 and higher when the sharing proportion is differentiated. In heavy load condition, as the efficiency of the converter is gradually decreasing, based on the above explanation, the system overall efficiency is lower when the sharing proportion is differentiated as shown in Fig. 4.

Accordingly, a system efficiency enhancement room exists especially under light load conditions. Special case is in medium load condition (I_{load} = 12A). The system power losses at k=0.1, k=1 and k=10 are almost the same, which means in medium load condition it becomes more viable to make converter equally share. But if the sharing proportion gain is further increased the system power losses can be reduced (see comparison between k=10 and k=100 in Fig. 4 (a)), which demonstrate that the system power losses can be changed by adjusting the sharing proportion.

Based on above discussion, by changing sharing proportion, the system efficiency can be improved under light to medium load conditions.

B. Effect of VR Shifting and Decision Variable

In order to change the current sharing proportion, an adaptive VR method is proposed, as shown in Fig. 5 (SVRC is not considered in this figure). Two converters are given the same reference voltage V_{ref}. Originally, the two converters share the load current equally (I_1=I_2=I_{load}/2). If the VR of one converter is changed to another value (see green line in Fig. 5), the sharing proportion is changed. Then, from (1) one can get:

$$I_j = \frac{V_{ref} - V_{DC}}{R_{dj}} \tag{8}$$

where I_j and R_{dj} are the output current and VR of the j^{th} converter respectively. In a 2-converter system, the load sharing ratio is:

$$\frac{I_1}{I_2} = \frac{R_{d2}}{R_{d1}} = k \tag{9}$$

Accordingly, the optimization objective is to find an optimal proportion of load current sharing by changing VR values. It is noteworthy that the ratio of the VR values determines the load current sharing proportion between units and consequently influences the system power loss, while the absolute values of VRs do not actually affect the system

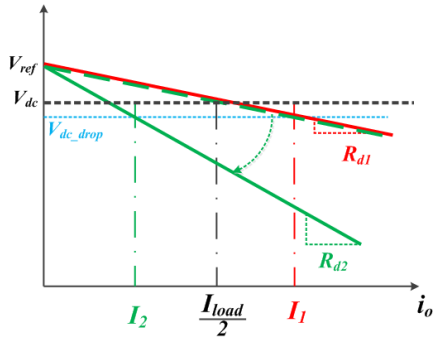

Fig. 5. Sharing Proportion Adjusting by VR Shifting

efficiency. It can be understood from Eq. (6) that the total power loss is decided by V_{DC}, I_j and η_j, if V_{DC} is kept at 48V by secondary control, η_j is determined by the converter feature and output current I_j (see Eq. (5)) Considering that the total output currents of all the converters are decided by the load current (see Eq. (7)), the change of VR values can only adjust the sharing proportion among converters (see Eq. (9)), while the absolute value of VR does not really affect the system efficiency. However, the VR changes certainly have influence on DC bus voltage (as can be seen from Fig. 5) and system dynamics. SVRC is necessarily needed to restore and stabilize the bus voltage. The system dynamics are analyzed and discussed in Section IV.

C. Optimization Problem Formulation

Based on the analysis above, the optimization problem can be described as:

$$Objective\_Function: Min\{P_{TL}\} \tag{10}$$

$$Decision\_Variables: \{R_{d1}, R_{d2}, ..., R_{dn}\} \tag{11}$$

$$Subject\_To: \begin{cases} 0 \le \{R_{d1}, R_{d2}, ..., R_{dn}\} \le 1 \\ \{I_1, I_2, ..., I_n\} \le I_{MAX} \\ I_1 + I_2 + ... + I_n = I_{load} \\ 1/20 \le k_{ij} \le 20 \end{cases} \tag{12}$$

$$Consider: \begin{cases} I_1 : I_2 : ... : I_n = \frac{1}{R_{d1}} : \frac{1}{R_{d2}} : ... : \frac{1}{R_{dn}} \\ \eta_j(I_j) = 0.975 \cdot e^{-2\times10^{-3}\cdot I_j} - 0.1257 \cdot e^{-0.3\cdot I_j} \end{cases} \tag{13}$$

where P_{TL} is the total power loss calculated by (6), R_d is the VR of each converter, as the optimization is actually to find an optimal sharing ratio, the given range of R_d is initially set to [0,1], I_{MAX} is the maximum conversion current limit of each converter, the sum of converter output current should be equal to total load current, and the ratio between any two converters (k_{ij}) is limited between 1/20 and 20.

According to (10)-(13), consider a system with two droop-controlled buck converters with same efficiency curve as shown in Fig. 3, under certain load current I_{load}, objective P_{TL} can be plotted with respect to VRs (R_{d1}, R_{d2}), which is shown in Fig. 6 (a)-(c). The shape and color represent the system power loss. The objective is to make the system operate in colder color and lower height areas.

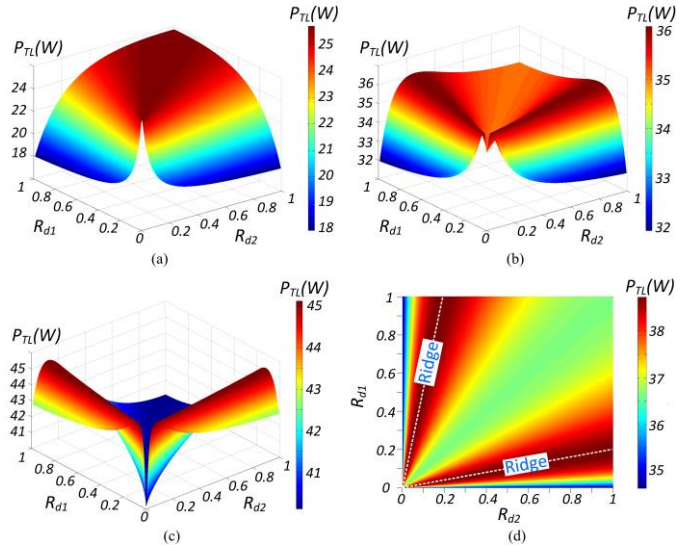

Fig. 6. Objective function plot with regard to virtual resistances: (a) objective function under I_{load}=6A; (b) objective function under I_{load}=12A; (c) objective function under I_{load}=15A; (d) contour view under I_{load}=13A.

According to Fig. 6 (a) and Fig. 6 (b), in light and medium load conditions it is more efficient to differentiate the VRs of two converters so as to make one of them supply most part of the load current. Considering the stability issues, the sharing ratio is limited between 1/20 to 20 instead of making some of them supplying all of the load current, as defined in (12). From another perspective, decision whether it is better to turn off the converter or keep it online depends on the characteristic of the consumption profile. If the load profile is stable during long time and changing slowly, one can just switch on and off some converters so as to enhance the efficiency [19], but if the load profile is dynamically changing, it is better to keep the converters online and VRs can be shifted to change the sharing as the case considered in this paper. In heavy load conditions as shown in Fig. 6 (c), it is better to set the same VRs so as to make them equally share the load current.

D. Optimization Algorithm Selection and Parameter Tuning

In order to solve the optimization model formulated above, a proper algorithm should be implemented. The selection of algorithms is based on the analysis of objective function. Global and local optimization methods are taken into option. The fastest optimization algorithms only seek local optimum point which is called local optimization, such as simplex method and gradient based algorithms. However, local optimization does not guarantee global optimal solution. On the other hand, global optimization algorithms, such as genetic algorithm (GA) and Particle Swarm Optimization (PSO), are able to find global optimum. However, they may require more computational time and memory space. Consequently, preliminary analysis and tests are necessary for selecting a proper algorithm and improving its performance.

It can be seen from Fig. 6 (d) that in this load condition there is a 'ridge' between two minimum sides. Different solutions may be obtained with different initial points. Local optimization is not capable of climbing over the 'ridge'.

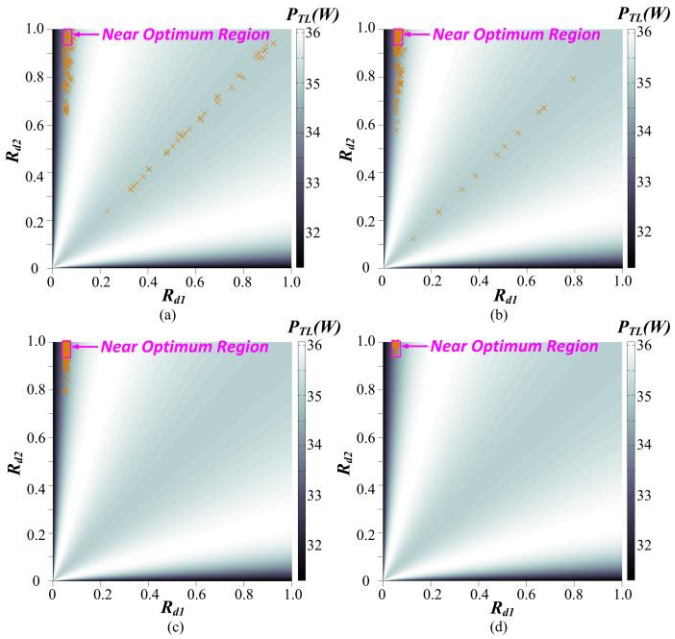

Fig. 7. GA Parameter Tuning: (a) N_{pop}=10, N_g=10; (b) N_{pop}=10, N_g=30; (c) N_{pop}=20, N_g=50; (d) N_{pop}=30, N_g=200.

Accordingly, this paper employs genetic algorithm to solve the optimization problem.

The basic parameters of GA significantly influence the performance of the program [30], [31]. For different sorts of problems, good parameter settings of GA can be significantly different. Parameter tuning and tests are necessary for ensuring that the algorithm gives reliable and optimal solutions.

When selecting parameters, such as population size (N_{pop}) and maximum number of generations (N_g), there is usually a tradeoff between computational time and quality of final solutions. In addition, as these parameters cannot be treated separately, a rational matching is also important.

In this paper, crossover rate is set to 0.8 (default setting), N_{pop} and N_g are tuned to achieve better performance. Case I_{load}*=12A* is used to adjust parameters because of the representativeness under this load condition, the algorithm is conducted 100 times to gather the final solutions (see Fig. 7). In order to use the least computational time while ensuring acceptable quality of final solutions, the tuning process starts from N_{pop} *=10*, N_g *=10* (see Fig. 7(a)).With this parameter setting, algorithm is not able to always put solutions into near-optimum region. To improve its performance, both N_{pop} and N_g are increased gradually (see Fig. 7(a)-(d)). Final settings (N_{pop} =30, N_g =200) are able to facilitate the solutions converge to the near-optimum region. Practically, GA finds a near global optimal solution in every situation.

In addition, consider that in a multi-converter system if the efficiencies of the converters are the same, in certain load conditions there will be multiple optimal solutions. The decision-making algorithm needs to decide which ones should supply most of the load current in certain load conditions. In this case, a scheduling procedure can be adopted, as it was done in i.e. [32]. A priority number can be assigned to each

converter deciding the operating sequence and distributing the total workload among all the converters over a period of time. But this approach is out of the scope of this paper.

IV. Secondary Control Scheme for System Damping

The dynamic model of a paralleled buck converter system (2 modules) is shown in Fig. 8. The droop control loop and secondary control loop is introduced in (1)~(4). VR appears as a proportional current feedback (R_{d1} and R_{d2}) over inner control loops. Voltage and current loops can be accomplished by conventional PI controllers:

$$\begin{aligned} i_{ref}(t) &= K_{Pv}\cdot\left(v_{DC}^{*}(t)-v_{DC}(t)\right)+K_{Iv}\cdot\int_0^t\left(v_{DC}^{*}(\tau)-v_{DC}(\tau)\right)d\tau \\ d(t) &= K_{Pc}\cdot\left(i_{ref}(t)-i_L(t)\right)+K_{Ic}\cdot\int_0^t\left(i_{ref}(\tau)-i_L(\tau)\right)d\tau \end{aligned} \tag{14}$$

where d is the duty ratio, i_L and v_{DC} are the converter inductor current and capacitor voltage respectively. K_{Pv}, K_{Pc}, K_{Iv} and K_{Ic} are the control parameters of voltage and current loop PI controllers, i_{ref} and v_{DC}^{*} are the references for current and voltage loops.

Based on Fig. 8, each converter can be described by the following dynamic model:

$$Plant:\begin{cases} L\dfrac{di_{L(j)}}{dt}=v_{in}\cdot d_{(j)}-v_{DC}-R_p\cdot i_{L(j)} \\ C\dfrac{dv_{DC}}{dt}=\displaystyle\sum_{j=1}^{N}i_{L(j)}-\frac{1}{R_{load}}\cdot v_{DC} \end{cases}$$

$$Controller:\begin{cases} d_{(j)}=\left(\dfrac{K_{Ic}}{s}+K_{Pc}\right)\cdot\left(i_{ref(j)}-i_{L(j)}\right) \\ i_{ref(j)}=\left(\dfrac{K_{Iv}}{s}+K_{Pv}\right)\cdot\left(v_{DC(j)}^{*}-v_{DC}\right) \\ v_{DC(j)}^{*}=v_{ref}-R_{d(j)}\cdot i_{L(j)} \\ v_{ref}=\left(\dfrac{K_{Isc}}{s}+K_{Psc}\right)\cdot\left(V_{ref}^{*}-v_{DC}\right)+V_{ref}^{*} \end{cases} \tag{15}$$

where subscript j denotes the j^{th} converter parameters, N is the total number of converters, L and C are inductance and capacitance of the converter output filter, R_p is the parasitic resistance of the filter, R_{load} is the equivalent resistance of the total load, v_{in} is the source voltage, v_{ref} is the common voltage reference generated by voltage secondary control, K_{Psc}, K_{Isc} and V_{ref}^{*} are the control parameters and reference of voltage secondary control loop.

In order to analyze a general multi-module system consisting of N converters, (14) has been rewritten in a more compact state space model defined as [23]:

$$\dot{x}_s = A_s\cdot x_s + B_s\cdot u \tag{16}$$

where all the modules share the common part of secondary control and capacitor. The eigenvalues of the state matrix A_s can be used to analyze system stability [23].

A. Root Locus Analysis

Based on the state space model (15), root locus can be obtained and used to examine the system dynamics. Inner loops are first tuned to achieve stable operation. VRs are then changed to obtain the root locus, as shown in Fig. 9. By changing the VRs with different ratios (k=1, k=2, k=5, k=20) in different load levels, the shifting trajectory of the system dynamics can be observed. According to efficiency curve in Fig. 3, when load current is smaller than 8-10A, it is more efficient to use only single converter, when load condition is in medium level, an optimal ratio can be found, while at heavy load condition, equally sharing load current is the most efficient way. Consequently, in Fig. 9, the root locus is obtained in different load levels, in light-load level (6A) k is set to 20, in medium-load level (12A) k is changed from 1 to 20 while in high-load level (20A) the k is set to 1.

Initially, in Fig. 9 (a)-(f), with all the eigenvalues located in the left-half plane (negative real part), the system is stable. However, the damping of the system should be constrained to a desired level. The minimum angle among all the eigenvalues actually represents the damping level of the system. As a result, in order to ensure that system operates with acceptable dynamic properties, the minimum angle of the eigenvalues can be controlled. Fig. 9 (a) shows the root locus under load current 6A, and the sharing ratio is 20:1 which means one converter supply the most load current. VR value of one converter is changed from 0.02-0.04, and the other from 0.4-0.8 to keep the sharing ratio. The roots marked by dashed circle which are sensitive to the VR value changing are the dominant poles affecting most the system damping. Similar phenomenon can be also observed in Fig. 9(b)-(e). As a conclusion, the purpose of Fig. 9 is to examine the system stability when change the VR value with different sharing ratio k. Fig. 9 (a)~(e) show the general root locus of the eigenvalues which indicate that the dominant eigenvalues are the ones that are marked by the dashed circle. The angle of these dominant eigenvalues (see the dashed line without arrow in Fig. 9 (f)) decides the damping level of the system. Consequently, the system damping can be controlled by constraining the minimum angle of the dominant eigenvalues by changing VRs of the converters with predefined ratio, as shown in Fig. 9(f) (the dominant eigenvalues can be controlled around the dashed line so as to obtain desirable system damping), while this ratio is actually the optimal ratio given by tertiary control.

To demonstrate the conclusion drawn above, the simulation results presented in Fig. 10 show the dynamic comparison for different VR settings with different sharing ratio k (e.g. k=1, 5,10). It can be observed that when increasing VR values, the minimal angle of eigenvalues is increasing, and the system becomes more damped. However, as can be seen from Eq. (1) that, if the VR value is set too large, it causes large transient deviation and long recovery time to the DC bus voltage during loading/unloading process (see blue curve of 'DC Bus Voltage' in Fig. 10). Accordingly, it is necessary to find the proper VR values so as to obtain desirable damping.

B. System Damping via Secondary Control

Although the VRs setting which offers better damping can be selected under a certain load condition according to system dynamic comparison as shown in Fig. 10. However, with the

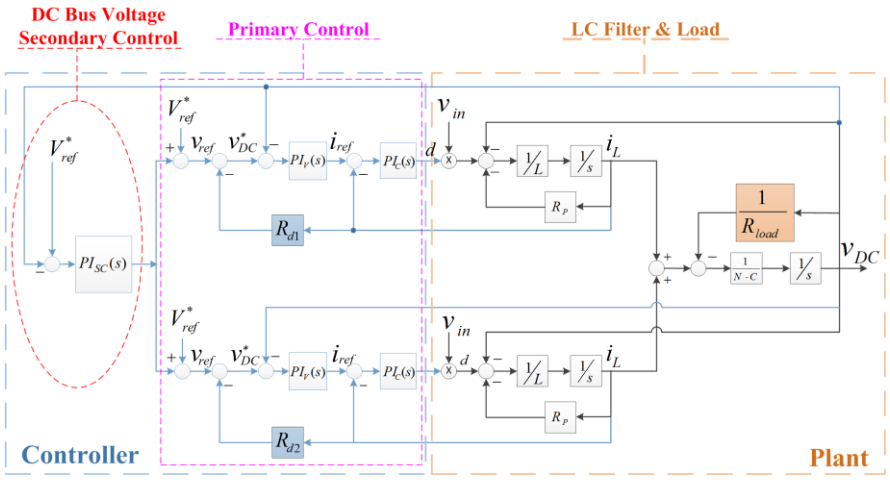

Fig. 8. Dynamic Model of a System with Two Paralleled Converters

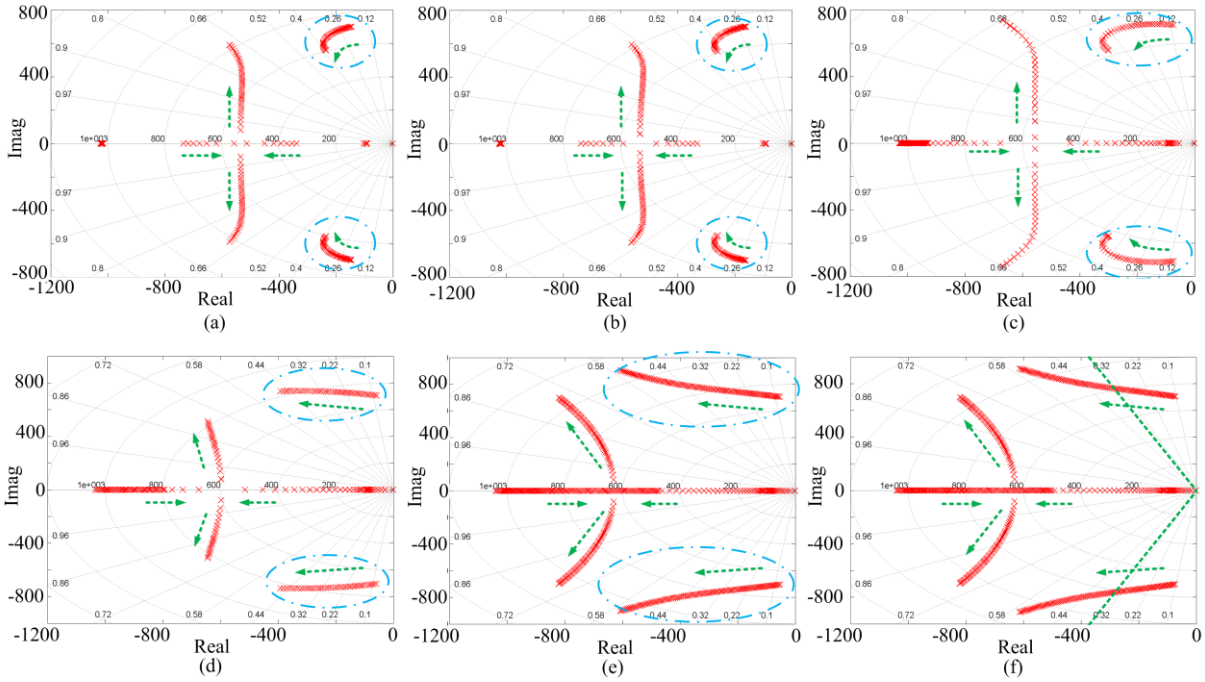

Fig. 9. Rootlocus of the system dynamic model with VR changing: (a) I_{load}=6A, k=20, R_{d1}=0.02-0.04, R_{d2}=0.4-0.8; (b) I_{load}=12A, k=20, R_{d1}=0.02-0.04, R_{d2}=0.4-0.8; (c) I_{load}=12A, k=5, R_{d1}=0.02-0.2, R_{d2}=0.1-1; (d) I_{load}=12A, k=2, R_{d1}=0.02-0. 4, R_{d2}=0.04-0.8; (e) I_{load}=12A, k=1, R_{d1}=0.02-1, R_{d2}=0.02-1; (f) I_{load}=20A, k=1, R_{d1}=0.02-1, R_{d2}=0.02-1.

fast changing of load condition as well as the readjustment of VRs from tertiary control, the desired VR values are also changing. Consequently, the best way to achieve desired system damping is to control the minimal angle of eigenvalues. Furthermore, tertiary control may be too slow for fast constraining system dynamics. Based on the discussion above, this paper proposes a SCSD, as shown in Fig. 11.

In this figure, the State Matrix Calculation block calculates the minimum angle of eigenvalues according to system state space model and system information (dc bus voltage, load condition, etc.). The minimum angle, $Angle_{min}$, is compared with a damping reference which is an angle value, the error is sent to a *PI* controller to adjust the initial value R_{d_ini}. Then, this value is multiplied by the optimal ratios (k_1, k_2, …, k_n) which are calculated according to TCEO solutions. Finally, the adjusted solutions are sent to primary controllers. LPFs are needed to smooth the shifting process.

It is worth noting that the range of VR values is not fixed. By applying SCSD, the optimal VR values from TCEO are automatically readjusted to ensure better system dynamics.

V. Hardware In the Loop Simulation Results

In order to validate the method presented in the paper, HIL simulations are conducted in dSPACE platform with exact models of four droop controlled dc-dc converters forming a dc conversion system. The electrical and control parameters are shown in Table I. The conversion system consists of four 100V/48V buck converters with maximum output current 20A of each. Assuming 10% of voltage regulation, all the VRs are set to 0.24 Ohm (according to (2)) so as to equally share load

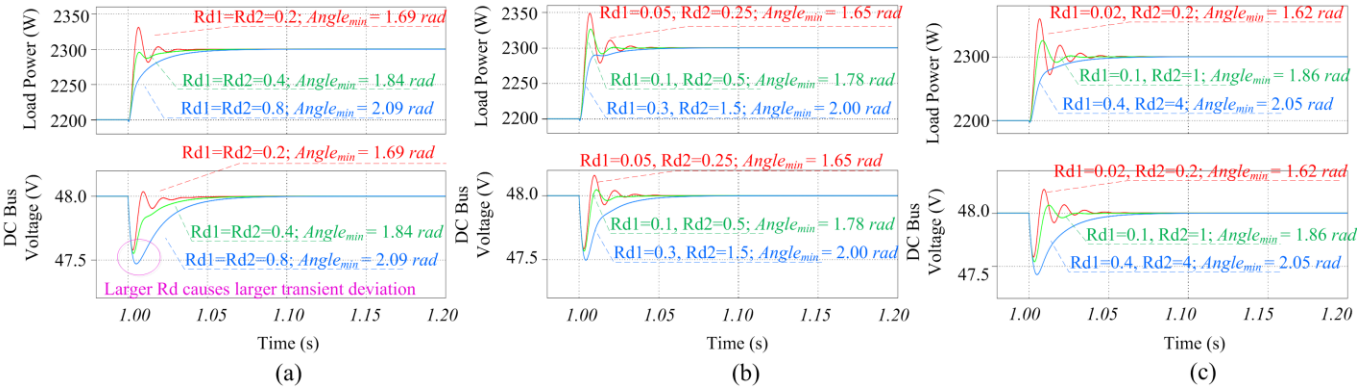

Fig. 10. System damping comparison with different VR ratio: (a) k=1, R_d changes from 0.2 to 0.8; (b) k=5, R_d changes from 0.05 to 1.5; (c) k=10, R_d changes from 0.02 to 4.

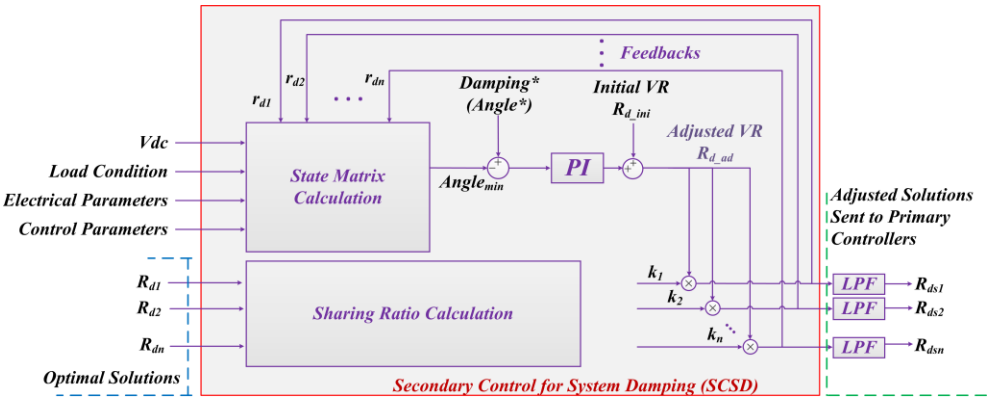

Fig. 11. Secondary control for system damping (SCSD).

TABLE I. ELECTRICAL AND CONTROL SYSTEM PARAMETERS

Class	Parameters	
Converter Basic	Converter Type	100V/48V Buck
	Max. Current	20 A (1000 W)
	Convertional Droop (R_d)	0.24 Ohm
	$Eff_{con1} > Eff_{con2} > Eff_{con3} > Eff_{con4}$	
Plant	L	1.8e^{-3} H
	C	2.2e^{-3} F
Primary Control (Inner Loop)	K_{Pc}	1
	K_{Ic}	97
	K_{Pv}	0.5
	K_{Iv}	993
	Time Step	1e^{-4}s
Voltage Secondary	K_{Psc}	0.02
	K_{Isc}	70
	Time Step	1e^{-4}s
Damping Secondary	K_{Pdp}	0.01
	K_{Idp}	20
	Damping(Angle*)*	1.95 rad
	Time Step	1e^{-4}s
Genetic Algorithm	N_{pop}	30
	N_g	400
	Time Step	2s

current. L and C are output filter inductor and capacitor equivalent values, K_{Pv}, K_{Pc}, K_{Psc}, K_{Pdp}, K_{Iv}, K_{Ic}, K_{Isc} and K_{Idp} are the proportional and integral term of voltage inner loop, current inner loop, voltage secondary control loop and SCSD loop, $Damping^*(Angle^*)$ is set to 1.95 rad, this value can be adjusted according to different system damping requirements. The cut-off frequency of the 1st order butterworth LPF implemented between SCSD and primary control is set to 5 Hz. And the four converters have small efficiency differences: converter 1 has the highest efficiency while converter 4 has the lowest. Three kinds of control methods are considered in this part: (m1) conventional fixed VR values, (m2) optimized sharing ratio without SCSD, (m3) optimized sharing ratio with SCSD. In Fig. 12, the system power loss and efficiency are compared between methods (m1) and (m3). Since SCSD does not affect the system efficiency and power loss, method (m2) is not presented in Fig. 12. The input load profiles in Fig. 12 are: (a) increasing load power from 200W to 3200W; (b) random load profile varying between 1000W and 3000W. Considering the system dynamic performance, the three methods (m1), (m2) and (m3) are compared in Fig. 16.

First, a simulation is conducted with load power increasing from 200W to 3200W, as shown in Fig. 12 (a). In the optimized system, the four converters are not always equally sharing load power, with the increasing of load power, the TCEO gradually increases the load sharing proportion of different converters. According to the power loss and efficiency comparison, the optimized control offers enhanced system efficiency improvement in light and medium load conditions while in heavy load condition, the room for optimization is limited. This result is in accordance with the objective function analysis done in Section III. Furthermore, during load power increasing, the dc bus voltage is stabilized to the rated value 48V. The current curves show the strategy of

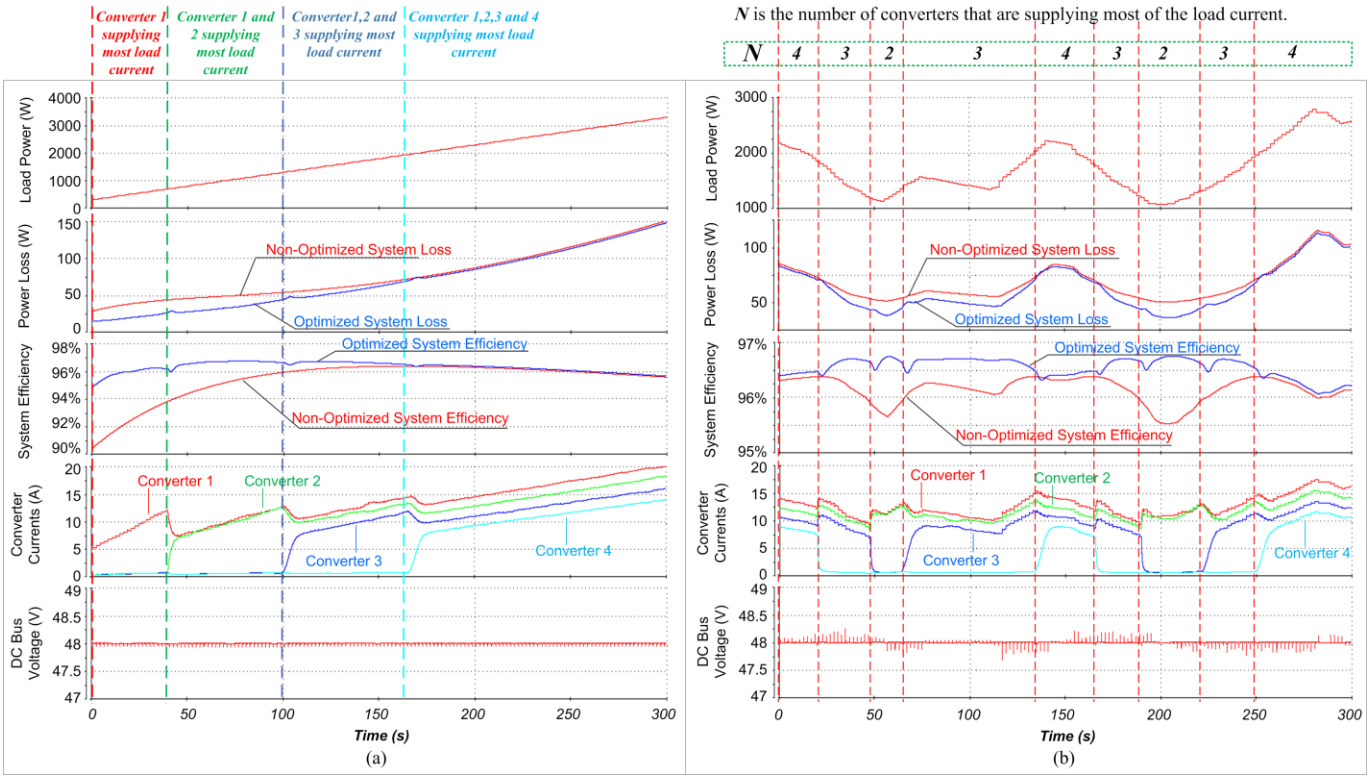

Fig. 12. HIL results: (a) with increasing load power; (b) with random generated load power.

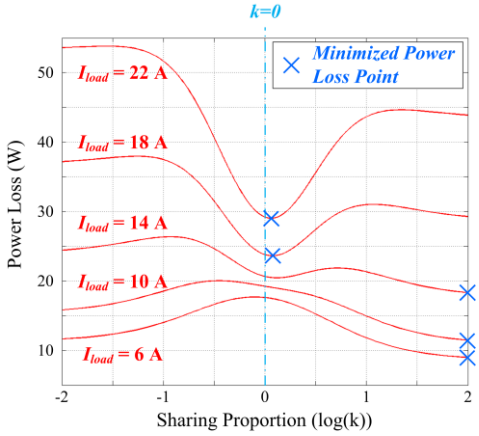

Fig. 13. System power loss (different efficiency features of converters are considered).

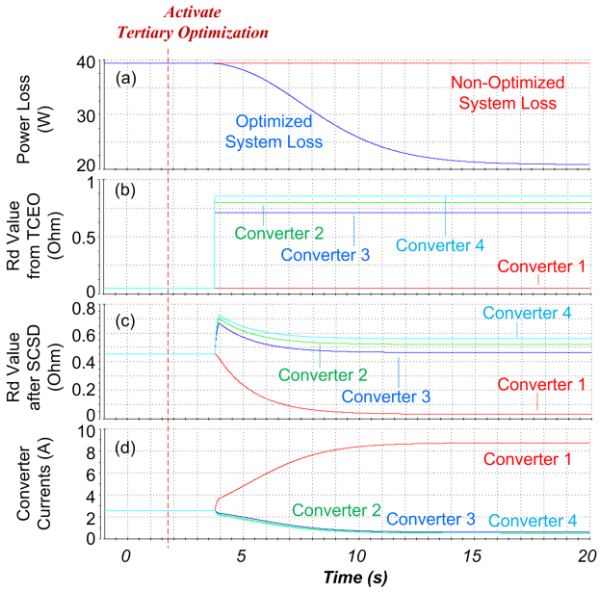

Fig. 14. Tertairy optimization performance.

employing converters in different load levels. Since converter 1 has the highest efficiency, it is most employed, while converter 4 has the lowest efficiency, it is the last considered converter. It is noteworthy that the converters which are not supplying current are not totally shut-down, they receive relative larger VR values from TCEO and also output small amount of current. In addition, the optimal load sharing ratio among units is achieved so as to maximize the overall efficiency.

One step further, in order to test the performance and response of the method under random load conditions, a load profile is given to the system, as shown in Fig. 12 (b). The load power is varying between 1000W and 3000W. During the test phase, it can be observed that the converter control strategy is optimized by the tertiary control and the system efficiency is enhanced compared with non-optimized results. In Fig. 12 (b), the parameter *N* is the number of converters that supply most of the load current, which denotes the decision given by tertiary control. In light load conditions when the TCEO employs less number of converters, the improvement of system efficiency is higher. In heavy load conditions, the four converters are supplying together with optimized sharing ratio.

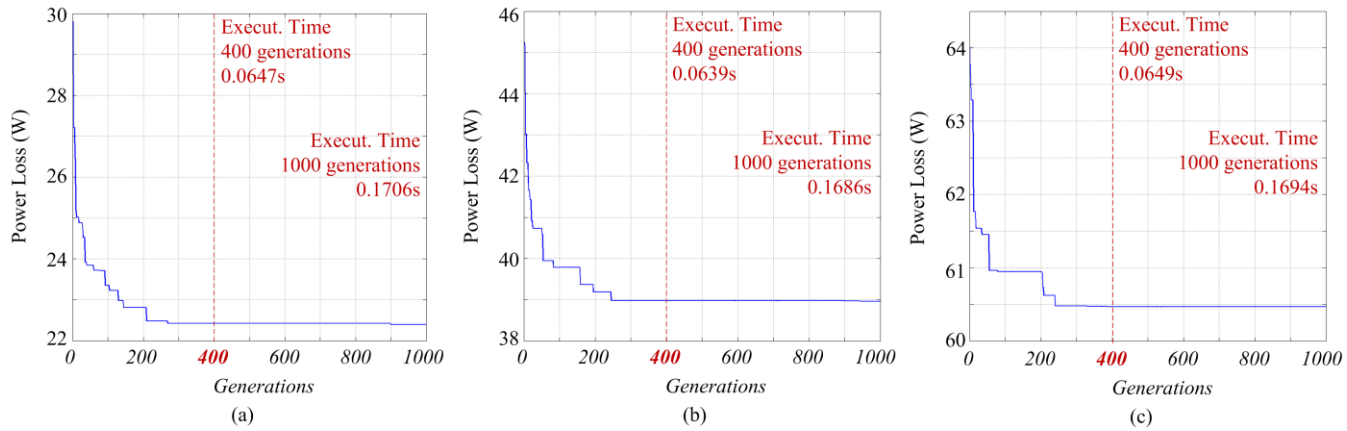

Fig. 15. Objective function value in each generation (in a 4-converter system): (a) light load condition, I_{load}=12A; (b) medium load condition, I_{load}=24A; (c) heavy load condition, I_{load}=36A.

Also, the dc bus voltage is kept at 48V throughout the test process by the secondary control action.

It needs to be clarified that, in light load conditions, the decision of which converters are heavily used and which are supplying small amount of current is also the solution given by TCEO. Moreover, the sharing proportion among heavily used converters is also optimized. It can be seen from Fig. 12 that, in medium load conditions (when converter1 and converter2 are supplying most of the load current), the difference of currents between converter1 and converter2 is not quite obvious, because in this condition, the optimized solution actually locates near equal sharing point. As shown in Fig. 13, the power loss is plotted considering two converters with different efficiency, and the blue cross points denote the minimized power loss point in different load conditions. When the load current is low, it is more efficient to increase the sharing proportion of the high efficiency converter. And when the load current is in medium level (18-22A), the minimized power loss point is near the equal sharing point, which results in the same output current of converter1 and converter2 when they are supplying most of the load current in Fig. 12. Furthermore, in heavy load conditions, the sharing proportion among all the converters is optimized according to their efficiency, result in the different output currents of all the converters. However, the optimization room is quite limited under this situation, so it does not improve much the system efficiency.

Considering the performance of the optimization algorithm, the detailed activation process is shown in Fig. 14. The load power is set to 500W, and at one point the TCEO is activated. After 2 seconds (one optimization time step), the TCEO finds a set of optimal R_d values, as that shown in Fig. 14 (b). Fig. 14 (c) shows the final R_d values which are readjusted by SCSD and LPF and then sent to primary controllers. By comparing Fig. 14 (b) and (c), it can be seen that the SCSD keeps the ratio between R_d values but adjusts the absolute values to ensure desirable system dynamics. Consequently the currents in Fig. 14 (d) are differentiated resulting in the reduced system power loss compared with non-optimized system (see Fig. 14 (a)). These results demonstrate that the TCEO is able to find

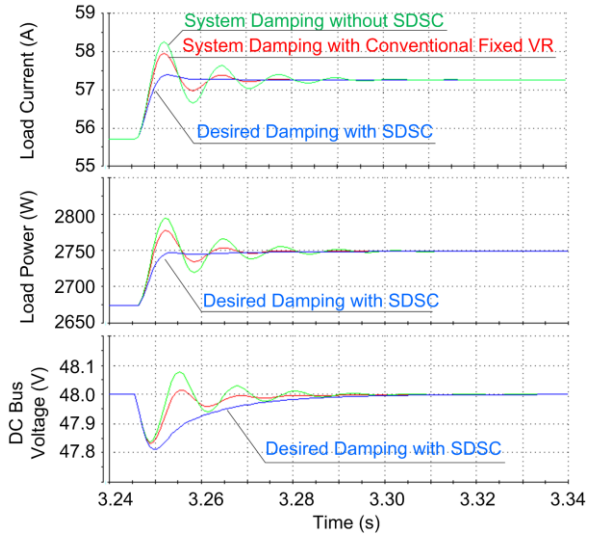

Fig. 16. System Dynamics Comparison

desirable solutions within pre-set times step (2s) and improve the efficiency of the system.

In order to show the performance of the optimization algorithm, the objective function value in each generation is plotted in Fig. 15 (in a 4-converter system with different load current level). 1000 generations are processed in each run, the total time consuming is 0.16~0.18s. It can be seen that in all load conditions, the GA tries to minimize the objective function value (power loss), and after 400 generations the optimization algorithm gives almost no improvements which indicates the convergence of GA to near optimal solution. Accordingly, the total number of generation (N_g) is set to 400 in this paper (see Table I). It takes 0.07~0.08s to process 400 generations in each run of GA.

In addition, it has to be clarified that this paper considers a constant input voltage (100V) to all the paralleled converters. If the input voltage is variable, a 3-dimension look-up table, which stores the efficiency value of the converter under different input voltages, can be used as the example case introduced in [18]. Considering that the aging of devices also influences the converter efficiency, online/offline efficiency

measurement can be deployed to refresh efficiency data and update the efficiency information periodically to improve the accuracy of the optimization results.

Apart from efficiency optimization, system dynamics are also important especially when varying VR values. The comparison among the ones with or without SCSD and with conventional fixed VRs is shown in Fig. 16. One can observe that the curve with SCSD shows improved system dynamics compared with the ones without SCSD. The load current and load power curves show that with SCSD, the current and power have a fast and more damped restoration after load changes. The voltage curve shows that SCSD limits the dc bus voltage oscillation after a load change.

VI. Conclusion

This paper proposes secondary and tertiary control levels for improving system dynamics and enhancing the efficiency of a paralleled dc-dc converter system. Conventionally, load current is equally shared among converters that the system efficiency is low, especially in light-load conditions. Hierarchical control conception is adopted and improved in this paper so as to realize system efficiency enhancement while ensure desirable system damping: (i) adaptive VR method is employed in the primary control level achieving proportionally adjustment of load sharing among converters and well interfacing with tertiary optimization; (ii) voltage secondary control takes charge of voltage deviation restoration, also a secondary control for system damping is proposed to improve the system dynamics; and (iii) GA is integrated in the tertiary level to enhance the system efficiency by solving an optimization problem, the system model is simplified formulating a proper mathematical model for optimization purpose, and online optimization is actualized.

HIL simulations are conducted in a system consisting of four buck converters with different efficiency characteristics. The results indicate the potential of the efficiency improvement in paralleled converter system. Also, the method is demonstrated to be capable of improving system efficiency while keeping desired system damping.

VII. References

[1] W. Chen, X. Ruan, H. Yan, and C. K. Tse, "DC/DC Conversion Systems Consisting of Multiple Converter Modules: Stability, Control, and Experimental Verifications," *IEEE Trans. Power Electron.*, vol. 24, no. 6, pp. 1463–1474, Jun. 2009.

[2] R. Ahmadi and M. Ferdowsi, "Improving the Performance of a Line Regulating Converter in a Converter-Dominated DC Microgrid System," *IEEE Trans. Smart Grid*, vol. 5, no. 5, pp. 2553–2563, Sep. 2014.

[3] B. G. Fernandes and S. Anand, "Modified droop controller for paralleling of dc–dc converters in standalone dc system," *IET Power Electron.*, vol. 5, no. 6, pp. 782–789, Jul. 2012.

[4] Y. Gu, X. Xiang, W. Li, and X. He, "Mode-Adaptive Decentralized Control for Renewable DC Microgrid With Enhanced Reliability and Flexibility," *IEEE Trans. Power Electron.*, vol. 29, no. 9, pp. 5072–5080, Sep. 2014.

[5] L. Xu and D. Chen, "Control and Operation of a DC Microgrid With Variable Generation and Energy Storage," *IEEE Trans. Power Deliv.*, vol. 26, no. 4, pp. 2513–2522, Oct. 2011.

[6] D. Salomonsson and A. Sannino, "Low-Voltage DC Distribution System for Commercial Power Systems With Sensitive Electronic Loads," *IEEE Trans. Power Deliv.*, vol. 22, no. 3, pp. 1620–1627, Jul. 2007.

[7] J. M. Guerrero, J. C. Vasquez, J. Matas, L. G. de Vicuna, and M. Castilla, "Hierarchical Control of Droop-Controlled AC and DC Microgrids—A General Approach Toward Standardization," *IEEE Trans. Ind. Electron.*, vol. 58, no. 1, pp. 158–172, Jan. 2011.

[8] A. Bidram and A. Davoudi, "Hierarchical Structure of Microgrids Control System," *IEEE Trans. Smart Grid*, vol. 3, no. 4, pp. 1963–1976, Dec. 2012.

[9] M. Farhadi and O. Mohammed, "Adaptive Energy Management in Redundant Hybrid DC Microgrid for Pulse Load Mitigation," *IEEE Trans. Smart Grid*, vol. PP, no. 99, pp. 1–1, 2014.

[10] T. Dragicevic, J. M. Guerrero, J. C. Vasquez, and D. Skrlec, "Supervisory Control of an Adaptive-Droop Regulated DC Microgrid With Battery Management Capability," *IEEE Trans. Power Electron.*, vol. 29, no. 2, pp. 695–706, Feb. 2014.

[11] W. Yu, H. Qian, and J. S. Lai, "Design of high-efficiency bidirectional DCDC converter and high-precision efficiency measurement," *IEEE Trans. Power Electron.*, vol. 25, pp. 650–658, 2010.

[12] A. V. Peterchev and S. R. Sanders, "Digital multimode buck converter control with loss-minimizing synchronous rectifier adaptation," *IEEE Trans. Power Electron.*, vol. 21, pp. 1588–1599, 2006.

[13] Q. Zhao and F. C. Lee, "High-efficiency, high step-up dc-dc converters," *IEEE Trans. Power Electron.*, vol. 18, pp. 65–73, 2003.

[14] K. C. Tseng and T. J. Liang, "Novel high-efficiency step-up converter," *IEE Proceedings - Electric Power Applications*, vol. 151. p. 182, 2004.

[15] M. D. Mulligan, B. Broach, and T. H. Lee, "A constant-frequency method for improving light-load efficiency in synchronous buck converters," *IEEE Power Electron. Lett.*, vol. 3, pp. 24–29, 2005.

[16] S. Musunuri and P. L. Chapman, "Improvement of light-load efficiency using width-switching scheme for CMOS transistors," *IEEE Power Electron. Lett.*, vol. 3, pp. 105–110, 2005.

[17] J. A. Abu-Qahouq, H. Mao, H. J. Al-Atrash, and I. Batarseh, "Maximum efficiency point tracking (MEPT) method and digital dead time control implementation," *IEEE Trans. Power Electron.*, vol. 21, pp. 1273–1280, 2006.

[18] D. Maksimovic and I. Cohen, "Efficiency Optimization in Digitally Controlled Flyback DC–DC Converters Over Wide Ranges of Operating Conditions," *IEEE Trans. Power Electron.*, vol. 27, no. 8, pp. 3734–3748, Aug. 2012.

[19] X. Yu, A. M. Khambadkone, H. Wang, and S. T. S. Terence, "Control of parallel-connected power converters for low-voltage microgrid - Part I: A hybrid control architecture," *IEEE Trans. Power Electron.*, vol. 25, pp. 2962–2970, 2010.

[20] S. Anand and B. G. Fernandes, "Reduced-Order Model and Stability Analysis of Low-Voltage DC Microgrid," *IEEE Trans. Ind. Electron.*, vol. 60, no. 11, pp. 5040–5049, Nov. 2013.

[21] E. Barklund, N. Pogaku, M. Prodanovic, C. Hernandez-Aramburo, and T. C. Green, "Energy management in autonomous microgrid using stability-constrained droop control of inverters," *IEEE Trans. Power Electron.*, vol. 23, pp. 2346–2352, 2008.

[22] R. Majumder, B. Chaudhuri, A. Ghosh, R. Majumder, G. Ledwich, and F. Zare, "Improvement of stability and load sharing in an autonomous microgrid using supplementary droop control loop," *IEEE Trans. Power Syst.*, vol. 25, pp. 796–808, 2010.

[23] P. Kundur, *Power System Stability and Control*, vol. 23. 2006, p. 739.

[24] V. Blasko and V. Kaura, "A new mathematical model and control of a three-phase AC-DC voltage source converter," *IEEE Trans. Power Electron.*, vol. 12, no. 1, pp. 116–123, 1997.

[25] A. J. Prabhakar, J. D. Bollinger, H. T. M. H. T. Ma, M. Ferdowsi, and K. Corzine, "Efficiency analysis and comparative study of hard and soft switching DC-DC converters in a wind farm," *2008 34th Annual Conference of IEEE Industrial Electronics*. pp. 2156–2160, 2008.

[26] Z. P. Z. Pan, F. Z. F. Zhang, and F. Z. Peng, "Power losses and efficiency analysis of multilevel dc-dc converters," *Twentieth Annual IEEE Applied Power Electronics Conference and Exposition 2005 APEC 2005*, vol. 3. pp. 1393–1398, 2005.

[27] M. Rafiq, F.-U.-H. Mohammed, M. Yaqoob, and T. Thiringer, "Analysis of power losses and efficiency up to 60 kW DC-DC converter for hybrid electric vehicle with different inductive core materials," in *2013 IEEE International Symposium on Industrial Electronics*, 2013, pp. 1–5.

[28] P. Klimczak and S. Munk-Nielsen, "Comparative study on paralleled vs. scaled dc-dc converters in high voltage gain applications," in *2008 13th International Power Electronics and Motion Control Conference*, 2008, pp. 108–113.
[29] W. W. W. Wu, X. W. X. Wang, P. G. P. Geng, and T. T. T. Tang, "Efficiency analysis for three phase grid-tied PV inverter," *2008 IEEE Int. Conf. Ind. Technol.*, 2008.
[30] J. J. Grefenstette, "Optimization of Control Parameters for Genetic Algorithms," *Syst. Man Cybern. IEEE Trans.*, vol. 16, pp. 122–128, 1986.
[31] S. Yussof and O. H. See, "The effect of GA parameters on the performance of GA-based QoS routing algorithm," in *Proceedings - International Symposium on Information Technology 2008, ITSim*, 2008, vol. 3.
[32] L. Meng, T. Dragicevic, J. M. Guerrero, and J. C. Vasquez, "Dynamic consensus algorithm based distributed global efficiency optimization of a droop controlled DC microgrid," in *2014 IEEE International Energy Conference (ENERGYCON)*, 2014, pp. 1276–1283.

VIII. BIOGRAPHIES

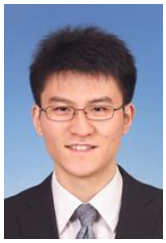

Lexuan Meng (S'13) received the B.S. degree in Electrical Engineering and M.S. degree in Electrical Machine and Apparatus from Nanjing University of Aeronautics and Astronautics (NUAA), Nanjing, China, in 2009 and 2012, respectively. He is currently working toward his Ph.D. in power electronic systems at the Department of Energy Technology, Aalborg University, Denmark, as part of the Denmark Microgrids Research Programme (www.microgrids.et.aau.dk).
His research interests include the energy management system, secondary and tertiary control for microgrids concerning power quality regulation and optimization issues, as well as the applications of distributed control and communication algorithms.

Tomislav Dragicevic (S'09-M'13) received the M.E.E. and the Ph.D. degree from the Faculty of Electrical Engineering, Zagreb, Croatia, in 2009 and 2013, respectively. Since 2010, he has been actively cooperating in an industrial project related with design of electrical power supply for remote telecommunication stations. Since 2013 he has been a fulltime Post-Doc at Aalborg University in Denmark. His fields of interest include modeling, control and energy management of intelligent electric vehicle charging stations and other types of microgrids based on renewable energy sources and energy storage technologies.

Juan C. Vasquez (M'12-SM'15) received the B.S. degree in Electronics Engineering from Autonomous University of Manizales, Colombia in 2004 where he has been teaching courses on digital circuits, servo systems and flexible manufacturing systems. In 2009, He received his Ph.D degree on Automatic Control, Robotics and Computer Vision from the Technical University of Catalonia, BarcelonaTECH, Spain at the Department of Automatic Control Systems and Computer Engineering, where he worked as Post-doc Assistant and also teaching courses based on renewable energy systems, and power management on ac/dc minigrids and Microgrids. Since 2011, he has been an Assistant Professor in Microgrids at the Department of Energy Technology, Aalborg University, Denmark, and he is co-responsible of the Microgrids research programme co-advising more than 10 PhD students and a number of international visitors in research experience. Dr Juan Vasquez is member of the Technical Committee on Renewable Energy Systems TC-RES of the IEEE Industrial Electronics Society and the IEC System Evaluation Group SEG 4 work on LVDC Distribution and Safety for use in Developed and Developing Economies. He is a visiting scholar at the Center for Power Electronics Systems – CPES at Virginia Tech, Blacksburg, VA, USA. He has published more than 100 journal and conference papers and holds a pending patent. His current research interests include operation, energy management, hierarchical and cooperative control, energy management systems and optimization applied to Distributed Generation in AC/DC Microgrids.

Josep M. Guerrero (S'01-M'04-SM'08-FM'15) received the B.S. degree in telecommunications engineering, the M.S. degree in electronics engineering, and the Ph.D. degree in power electronics from the Technical University of Catalonia, Barcelona, in 1997, 2000 and 2003, respectively. Since 2011, he has been a Full Professor with the Department of Energy Technology, Aalborg University, Denmark, where he is responsible for the Microgrid Research Program. From 2012 he is a guest Professor at the Chinese Academy of Science and the Nanjing University of Aeronautics and Astronautics; from 2014 he is chair Professor in Shandong University; and from 2015 he is a distinguished guest Professor in Hunan University.
His research interests is oriented to different microgrid aspects, including power electronics, distributed energy-storage systems, hierarchical and cooperative control, energy management systems, and optimization of microgrids and islanded minigrids. Prof. Guerrero is an Associate Editor for the IEEE TRANSACTIONS ON POWER ELECTRONICS, the IEEE TRANSACTIONS ON INDUSTRIAL ELECTRONICS, and the IEEE Industrial Electronics Magazine, and an Editor for the IEEE TRANSACTIONS on SMART GRID and IEEE TRANSACTIONS on ENERGY CONVERSION. He has been Guest Editor of the IEEE TRANSACTIONS ON POWER ELECTRONICS Special Issues: Power Electronics for Wind Energy Conversion and Power Electronics for Microgrids; the IEEE TRANSACTIONS ON INDUSTRIAL ELECTRONICS Special Sections: Uninterruptible Power Supplies systems, Renewable Energy Systems, Distributed Generation and Microgrids, and Industrial Applications and Implementation Issues of the Kalman Filter; and the IEEE TRANSACTIONS on SMART GRID Special Issue on Smart DC Distribution Systems. He was the chair of the Renewable Energy Systems Technical Committee of the IEEE Industrial Electronics Society. In 2014 he was awarded by Thomson Reuters as Highly Cited Researcher, and in 2015 he was elevated as IEEE Fellow for his contributions on "distributed power systems and microgrids."